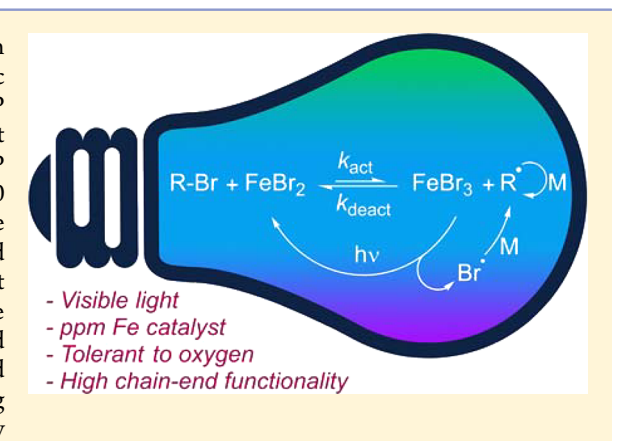
Photoinduced Iron-Catalyzed Atom Transfer Radical Polymerization with ppm Levels of Iron Catalyst under Blue Light Irradiation

Sajjad Dadashi-Silab, † Niangcheng Pan, † and Krzysztof Matyjaszewski*,† and Krzysztof Matyjaszewski

Supporting Information

200433, China

ABSTRACT: Photoinduced atom transfer radical polymerization (ATRP) has been mainly explored using copper-based catalytic systems. Recently developed iron-catalyzed photochemical ATRP employed high amounts of iron catalysts under high-energy UV light irradiation. Herein, a successful photoinduced iron-catalyzed ATRP mediated under blue light irradiation with ppm amounts (100-400 ppm) of iron(III) bromide/tetrabutylammonium bromide as the catalyst is reported. Several methacrylate monomers were polymerized with excellent control providing molecular weight in good agreement with theoretical values and low dispersity (D < 1.20). Near-quantitative monomer conversions (~95%) enabled in situ chain extension and block copolymerization, indicating high retention of chain-end functionality. Notably, this system can tolerate oxygen, enabling synthesis of well-defined polymers with good chain-end functionality in the presence of air.



■ INTRODUCTION

The evolution of reversible deactivation radical polymerization (RDRP) techniques has led to the synthesis of well-defined polymers with predetermined molecular weight, incorporated functionality, and complex architecture from a broad range of radically (co)polymerizable monomers. Atom transfer radical polymerization (ATRP), 1-5 reversible addition—fragmentation chain transfer (RAFT), and nitroxide-mediated polymerization (NMP)⁷⁻⁹ are the most widely explored RDRP techniques for the controlled synthesis of polymers.

In ATRP, a transition metal catalyst is used to establish and maintain a dynamic equilibrium between dormant and active species resulting in a well-controlled polymerization. 10 Copper complexes (Cu/L) are the most commonly used catalysts in ATRP reactions. 11 Initially, in a procedure known as normal ATRP, large amounts of catalyst were used in order to compensate for irreversible radical termination reactions that resulted in buildup of the higher oxidation state deactivator catalyst species. Recent developments in ATRP techniques have been directed toward designing new catalytic systems that can minimize catalyst loadings by in situ (re)generation of the activator species. For instance, thermal radical initiators can be used to slowly form radicals that react with CuII/L to regenerate Cu^I/L species in a procedure known as initiators for continuous activator regeneration (ICAR) ATRP. 12,13 Chemical reducing agents are used in activators regenerated by electron transfer (ARGET) ATRP. 12,14,15 Zerovalent metals can be used in heterogeneous manner in supplemental activator and reducing agents (SARA) ATRP. 16-19 Applying external stimuli offers the opportunity to mediate and control polymerization in a spatiotemporal manner, in addition to regeneration of the activator catalyst. To that end, the use of electrical current (eATRP), 20-24 light, 25-33 and ultrasound 34,35 have recently been developed for ATRP. These methods can be employed for activator regeneration under mild conditions while eliminating some side reactions that could be observed with the use of chemical reducing agents.

Photochemistry has the potential to simplify reaction setup, conduct reactions under mild conditions, and offer spatial and temporal control over the polymerization. 36-41 Photochemical ATRP has been the focus of intense research in recent years using primarily Cu^{II}/L complexes. Mechanistically, it was shown that photoinduced electron transfer reactions between the electron donors and Cu^{II} species result in the activator (re)generation. Recently, photoredox catalysis, which is based on utilization of either a transition metal-based photocatalyst^{32,42} or an organocatalyst⁴³⁻⁴⁸ to drive forward ATRP reactions, has seen a surge in interest for photochemical ATRP. In photoredox ATRP, excitation of the photocatalyst under light generates a highly reducing species that can reduce the alkyl halide initiator to form initiating radicals, which can be

Received: August 7, 2017 Revised: September 18, 2017 Published: October 5, 2017

[†]Department of Chemistry, Carnegie Mellon University, 4400 Fifth Avenue, Pittsburgh 15213, Pennsylvania United States [‡]State Key Laboratory of Molecular Engineering of Polymers, Department of Macromolecular Science, Fudan University, Shanghai

deactivated in a photocatalytic cycle to assert control over the polymerization reaction.

Iron (Fe) represents an environmentally benign opportunity to replace Cu catalysts or other precious metal-based complexes in catalyzing ATRP. ^{49–53} It is one of the most abundant metals on the planet and promotes many biological processes. As such, Fe is of great importance for a wide array of chemical reactions and applications as it provides low toxicity, biocompatibility, and cost-effectiveness.⁵⁴ A variety of Fe-based catalytic systems have been developed using ligands containing nitrogen⁵⁵ and phosphorus section compounds or halide anions. 62-64 Moreover, Fe-catalyzed ATRP can be controlled in the absence of additional ligands with polar solvents acting as complexing ligands. 65 Fe-based photochemical ATRP was shown to initiate and control polymerization of methacrylate monomers under UV light.⁶⁶ It was proposed that in the presence of methyl methacrylate (MMA) FeBr₃ could be photochemically reduced to the FeBr₂ activator species, which in turn also resulted in bromination of the MMA monomer. This process could also proceed in the absence of additional ligands in polar solvents, such as acetonitrile or dimethylformamide, solubilizing the Fe species. The brominated MMA (methyl 2,3-dibromoisobutyrate) formed during the photoreduction of FeBr3 is an alkyl halide species capable of initiating polymerization, and this was further taken advantage of in the polymerization of MMA in the absence of ATRP initiators and ligands. 48,67 Furthermore, iron(III) chloride-mediated systems have been studied.6 Nitrogen and phosphorus-based ligands were shown to be efficient in photochemical Fe ATRP reactions. However, the majority of photoinduced Fe-catalyzed ATRP systems reported so far have used high concentrations of Fe catalysts under highenergy UV light irradiation. Moreover, Fe photoredox complexes possessing low excited state lifetime have been proven less efficient in photoredox ATRP.68

In this paper, we show that photoinduced Fe-catalyzed ATRP can be conducted in a controlled manner under a wide range of light sources from UV to blue and even to green light LEDs. The versatility of this system allows decreasing the concentration of the Fe catalyst to ppm levels while providing controlled polymerization of several methacrylate monomers. The system was used to form block copolymers *in situ*, which is indicative of the preservation of high chain-end functionality. Furthermore, the polymerization of MMA can be successfully conducted in nondegassed solutions, i.e., in the presence of oxygen.

■ RESULTS AND DISCUSSION

Photoinduced Fe-Catalyzed ATRP: Optimization of Conditions. Originally, photoinduced Fe-catalyzed ATRP occurred in the presence of high catalyst loadings only under relatively high energy light sources such as UV light. Therefore, we decided to investigate the Fe-based catalysts for ATRP under visible light irradiation while decreasing the catalyst content to ppm levels. Control experiments were performed in a systematic manner to elucidate the influence and contribution of each component involved in the reaction and optimize reaction conditions.

Polymerization of methyl methacrylate (MMA) in anisole was studied using ethyl α -bromophenylacetate (EBPA) as the initiator, FeBr $_3$ as the catalyst, and tetrabutylammonium bromide (TBABr) as the ligand. In the absence of EBPA initiator, with FeBr $_3$ /TBABr at 100 ppm with respect to monomer (entry 1, Table 1), the reaction resulted in <4%

Table 1. Photoinduced Fe-Catalyzed ATRP of MMA^a

entry	[MMA]/[EBPA]/ [FeBr ₃]/[TBABr]	time (h)	conv (%)	$M_{ m n,th}$	$M_{ m n}$	Ð
1	100/0/0.01/0.01	16	<4		33000	1.60
2	100/1/0.01/0	16	37	3950	13400	5.15
3 ^b	100/1/0.01/0.01	38				
4	100/1/0.01/0.01	10	93	9550	10300	1.32
5	100/1/0.02/0.02	12	92	9450	9400	1.22
6	100/1/0.04/0.04	16	94	9650	10500	1.17
7	100/0/0.1/0.1	16	33		40000	1.43
8	100/1/0.1/0.1	16	73	7550	7700	1.18
9	100/1/1/0	96	75	7750	7100	1.79
10	100/0/1/1	96	10		2750	1.17
11	100/1/1/1	96	40	4250	3200	1.13

"Reactions were conducted in 50 vol % anisole, irradiated under blue light LED (λ = 450 nm, 4 mW/cm²). Conversions were calculated by ¹H NMR. Theoretical molecular weight ($M_{\rm n,th}$) values were calculated based on conversions as $M_{\rm n,th} = M_{\rm EBPA} + [{\rm MMA}]/[{\rm EBPA}] \times {\rm conversion} \times M_{\rm MMA}$. Number-average molecular weight ($M_{\rm n}$) and dispersity (D) were obtained by size exclusion chromatography (SEC) in THF based on poly(methyl methacrylate) standards. ^bReaction was kept in the dark.

monomer conversion after 16 h irradiation under blue light LED irradiation (λ = 450 nm, 4 mW/cm²) with number-average molecular weight ($M_{\rm n}$) of 33 000 and a relatively high dispersity (D) of 1.6. EBPA and 100 ppm FeBr₃, but without TBABr resulted in no control over the polymerization with molecular weight higher than theoretical value ($M_{\rm n,th}$ = 3950 vs $M_{\rm n}$ = 13 400) and D of 5.15 (entry 2, Table 1). Moreover, no polymerization was observed after 38 h when the reaction was kept in the dark (entry 3, Table 1). These results indicated the importance of the initially added ATRP initiator and the ligand in a polymerization using ppm levels of FeBr₃ catalyst as well as light source for a successful controlled polymerization.

As shown in entries 4–6, Table 1, reactions proceeded in a well-controlled manner in the presence of 100, 200, and 400 ppm of FeBr₃/TBABr under blue light LED irradiation, respectively. The rate of the reaction decreased as the concentration of FeBr₃ was increased (see next section for detailed discussion of kinetics results), but high or near-quantitative monomer conversions were achieved with low *D*. In a reaction with 1000 ppm FeBr₃/TBABr and in the absence of EBPA initiator (entry 7, Table 1), slightly better control was achieved compared to the 100 ppm FeBr₃/TBABr without EBPA (entry 1, Table 1). As expected, increasing the concentration of FeBr₃ to 1000 ppm resulted in a greater decrease in the rate of the reaction, 73% monomer conversion after 16 h irradiation (entry 8, Table 1).

Moreover, further increasing the concentration of FeBr₃ to equimolar ratios with respect to initiator (10 000 ppm) resulted in a significant decrease in the rate of the reaction. The reaction in the absence of the ligand (entry 9, Table 1) proceeded slightly faster than those in the presence of TBABr (entry 11, Table 1). However, good control was achieved using TBABr as the ligand in terms of low dispersity (D = 1.13 vs 1.79). The presence of TBABr was necessary for stabilization of FeBr₃ and/or FeBr₂ species in a nonpolar solvent such as anisole and hence controlling the polymerization process. Polymerization of MMA in the absence of EBPA, using 10 000 ppm FeBr₃/TBABr, was even slower, and it reached only 10% monomer conversion after 96 h irradiation under blue LEDs (entry 10, Table 1). Finally, in the presence of EBPA initiator with an

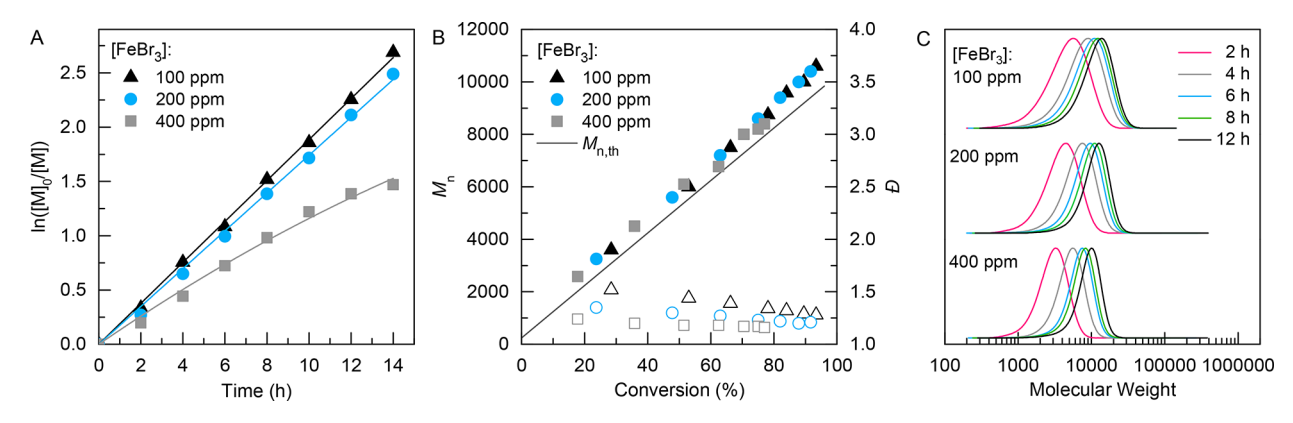


Figure 1. Photoinduced Fe-catalyzed ATRP of MMA under UV light irradiation (λ = 365 nm, 6 mW/cm²). (A) Kinetics of the polymerization. (B) Number-average molecular weight (M_n , solid points) and dispersity (D, open points) as a function of monomer conversion. (C) SEC traces for the PMMA synthesized with different catalyst loadings. Reaction conditions: [MMA]/[EBPA]/[FeBr₃]/[TBABr] = 100/1/x/x in anisole 50 vol % (x = 0.01, 0.02, and 0.04).

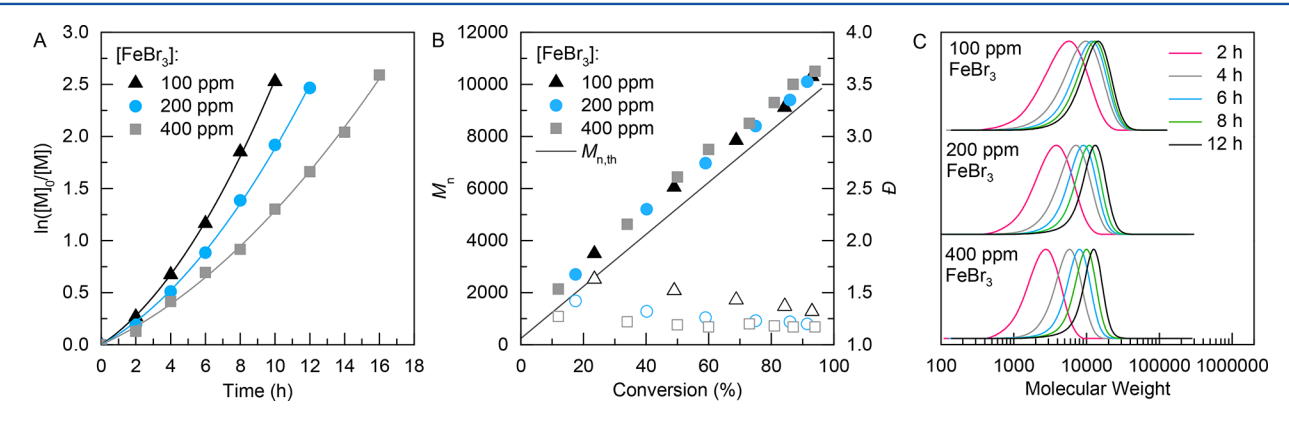


Figure 2. Photoinduced Fe-catalyzed ATRP of MMA under blue light LED irradiation (λ = 450 nm, 4 mW/cm²). (A) Kinetics of the polymerization. (B) Number-average molecular weight ($M_{\rm n}$, solid points) and dispersity (D, open points) as a function of monomer conversion. (C) SEC traces for the PMMA synthesized with different catalyst loadings. Reaction conditions: [MMA]/[EBPA]/[FeBr₃]/[TBABr] = 100/1/x/x in anisole 50 vol % (x = 0.01, 0.02, and 0.04).

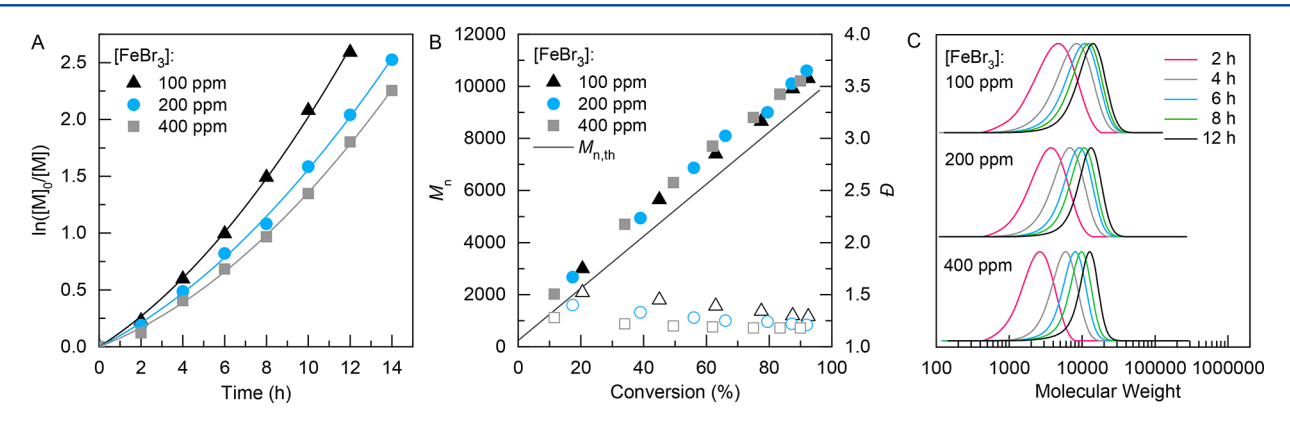


Figure 3. Photoinduced Fe-catalyzed ATRP of MMA under blue light LED irradiation (λ = 450 nm, 4 mW/cm²) in the presence of excess ligand. (A) Kinetics of the polymerization. (B) Number-average molecular weight (M_n , solid points) and dispersity (D, open points) as a function of monomer conversion. (C) SEC traces for the PMMA synthesized with different catalyst loadings. Reaction conditions: [MMA]/[EBPA]/[FeBr₃]/[TBABr] = 100/1/x/6x in anisole 50 vol % (x = 0.01, 0.02, and 0.04).

equimolar ratio of FeBr₃, the reaction reached to 40% monomer conversion after 96 h irradiation (entry 11, Table 1).

Kinetics of Photoinduced Fe-Catalyzed ATRP. After the reaction conditions were optimized, the kinetics of the polymerization of MMA was investigated using 100, 200, and 400 ppm FeBr₃/TBABr catalyst. Broad absorption spectra of FeBr₃/TBABr allow for controlling the polymerization using light sources with a variety of wavelengths. Different light

sources used to initiate reactions, included a UV lamp at $\lambda = 365$ nm (6 mW/cm²), blue light LEDs at $\lambda = 450$ nm (4 mW/cm²), and green light LEDs at $\lambda = 520$ nm (2.5 mW/cm²). Figure 1 shows the kinetics of the polymerization of MMA under UV light ($\lambda = 365$ nm, 6 mW/cm²) irradiation. Linear semilogarithmic kinetic plots were observed at various FeBr₃/TBABr concentrations with molecular weights increasing as a function of monomer conversion.

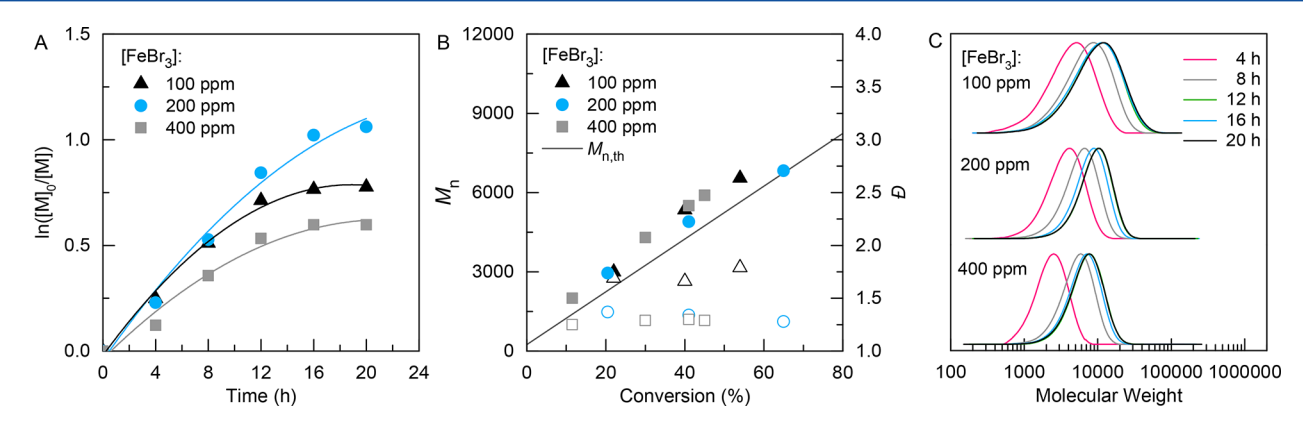


Figure 4. Photoinduced Fe-catalyzed ATRP of MMA under green light LED irradiation (λ = 520 nm, 2.5 mW/cm²). (A) Kinetics of the polymerization. (B) Number-average molecular weight ($M_{\rm n}$, solid points) and dispersity (D, open points) as a function of monomer conversion. (C) SEC traces for the PMMA synthesized with different catalyst loadings. Reaction conditions: [MMA]/[EBPA]/[FeBr₃]/[TBABr] = 100/1/x/x in anisole 50 vol % (x = 0.01, 0.02, and 0.04).

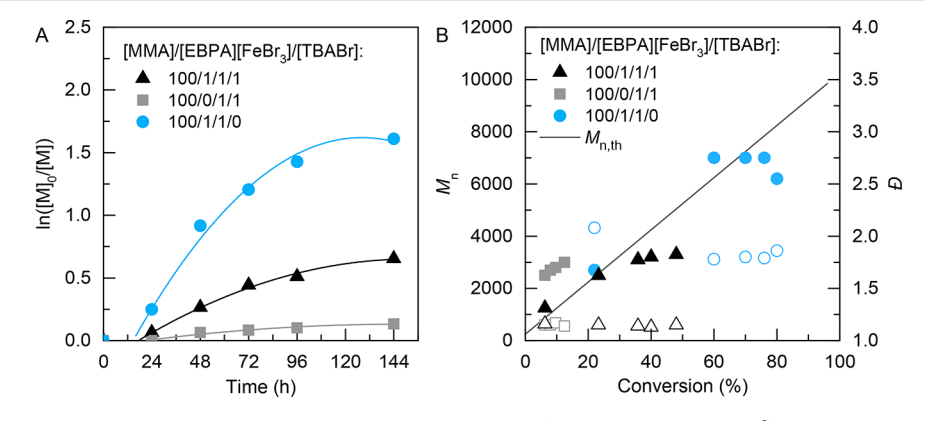


Figure 5. Photoinduced Fe-catalyzed ATRP of MMA under blue LED irradiation (λ = 450 nm, 4 mW/cm²) using equimolar ratios of FeBr₃ catalyst under different conditions. (A) Kinetics of the polymerization and (B) number-average molecular weight ($M_{\rm n}$, solid points) and dispersity (D, open points) as a function of monomer conversion.

Table 2. Photoinduced Fe-Catalyzed ATRP of MMA in the Presence of Oxygen^a

entry	$[\mathrm{MMA}]/[\mathrm{EBPA}]/[\mathrm{FeBr_3}]/[\mathrm{TBABr}]$	degassed	time (h)	conv (%)	$M_{ m n,th}$	$M_{ m n}$	Đ
1	100/1/0.04/0.04	no	28	93	9550	10000	1.38
2	100/1/0.04/0.04	yes	16	94	9650	10500	1.17
3	100/1/0.1/0.1	no	36	88	9150	8900	1.20
4	100/1/0.1/0.1	yes	32	91	9350	8900	1.18

^aReactions were conducted in 50 vol % anisole and irradiated under blue light LEDs (λ = 450 nm, 4 mW/cm²).

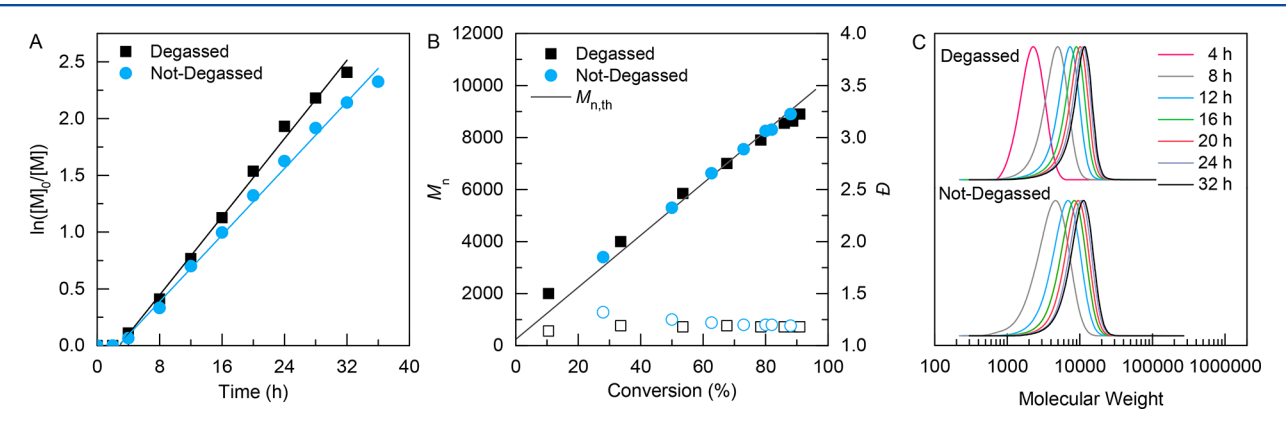


Figure 6. Photoinduced Fe-catalyzed ATRP of MMA under blue LED (λ = 450 nm, 4 mW/cm²) in degassed and nondegassed solutions. (A) Kinetics of the polymerization and (B) number-average molecular weight ($M_{\rm n}$, solid points) and dispersity ($D_{\rm n}$, open points) as a function of monomer conversion the PMMA synthesized with different catalyst loading. Reaction conditions: [MMA]/[EBPA]/[FeBr₃]/[TBABr] = 100/1/0.1/0.1 in anisole (50 vol %).

Table 3. Polymerization of MMA with Varying Degrees of Polymerization Using FeBr₃ under Blue Light LED Irradiation^a

entry	target DP	time (h)	conv (%)	$M_{ m n,th}$	$M_{\rm n}$	Đ
1	25	24	92	2550	2800	1.18
2	50	22	94	5000	5350	1.17
3	100	16	94	9950	10500	1.17
4	200	14	93	18850	18900	1.25

 a [MMA]/[EBPA]/[FeBr₃]/[TBABr] = x/1/0.04/0.04 (x = 25, 50, 100, 200) in 50 vol % anisole.

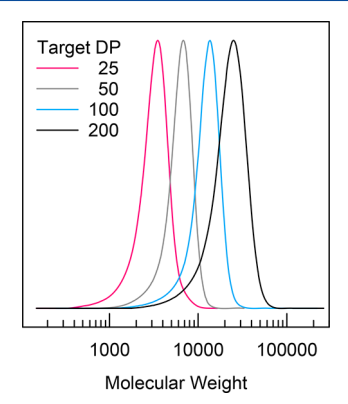


Figure 7. SEC traces for various degrees of polymerization (DP) in the photoinduced Fe-catalyzed ATRP under conditions: [MMA]/[EBPA]/[FeBr₃]/[TBABr] = x/1/0.04/0.04 (x = 25, 50, 100, 200) in 50 vol % anisole under blue light irradiation.

The reaction proceeded in a similar fashion using the blue light LEDs with the rate of the reaction decreasing with increasing FeBr₃ concentration from 100 to 200 and 400 ppm (Figure 2). Depending on the concentration of the catalyst, reactions reached high or near-quantitative monomer conversions within 10–16 h irradiation under blue light LEDs. In all cases, molecular weights were in good agreement with theoretical values and displayed low *D*, in the range of 1.17–1.30. Moreover, the reaction was examined in the presence of excess amounts of TBABr ligand, at a ratio of [FeBr₃]/[TBABr] = 1/6. As shown in Figure 3, though not significantly, the rate of the reaction decreased slightly compared to the reaction with an equimolar ratio of the ligand. Nevertheless, in both equimolar and excess ratios of the ligand, reactions proceeded in a well-controlled manner.

The kinetics of the polymerization of MMA were also investigated using green light LEDs (λ = 520 nm, 2.5 mW/cm²). As presented in Figure 4, the rate of the reaction with green LEDs was slower compared to those conducted under blue LEDs. This could be attributed to the fact that the absorption of the catalyst is maximized in blue region of the electromagnetic spectrum with a tailing absorption extending to the green region. The efficiency of green LEDs was not as high in the polymerization of MMA in blue LEDs or under a UV lamp. Monomer conversions were limited to 50–60% whereas in other cases near-quantitative conversions were reached regardless of the FeBr₃ ratio, and quite high D in the range of 1.30–1.80 were obtained under green light LEDs.

To illustrate the efficiency of the photoinduced Fe-catalyzed ATRP with ppm level catalyst under blue light irradiation, the kinetics of the polymerization of MMA were investigated using an equimolar ratio of FeBr₃ with respect to initiator. The results are shown in Figure 5. Because of the high concentration of the

deactivator initially present, the reactions proceeded at a much lower rate of polymerization compared to previous results obtained in the presence of ppm FeBr₃ catalyst (Figure 2). An induction period of 16-18 h was observed, indicating that in the presence of high amounts of FeBr₂ it took a longer time to build up a sufficient concentration of activator FeBr₂ species to initiate the reaction. In the absence of TBABr ligand, the reaction with $[MMA]/[EBPA]/[FeBr_3] = 100/1/1$ was not well-controlled. Monomer conversion reached 80% within 144 h irradiation under blue LEDs with quite high \mathcal{D} in the range 1.80-2.08. Including TBABr in the reaction medium resulted in a decrease in the rate of the reaction, but a well-controlled polymerization was achieved. However, when reaching higher conversions, a deviation of the molecular weights from theoretical values was observed under these reaction conditions: $[MMA]/[EBPA]/[FeBr_3]/[TBABr] = 100/1/1/1$. This could be attributed to the in situ formation of an alkyl halide initiator as a result of the bromination of MMA through photoreduction of FeBr₃ over time, as previously reported.⁶⁶ Nevertheless, polymerization was well-controlled with \mathcal{D} as low as 1.14. In the absence of EBPA, the reaction was even slower with 10% monomer conversion observed after 144 h irradiation under blue light generating a polymer with low \mathcal{D} (1.14).

Scope of the Photoinduced Fe-Catalyzed ATRP. Oxygen Reduction. The presence of oxygen is often detrimental in radical polymerizations as oxygen quenches initiating/growing radicals, generating inactive peroxy radical species. Photochemistry is an efficient approach to overcome oxygen inhibition problems in polymerizations, especially in RDRP techniques. For example, Cu-based photoinduced ATRP can proceed in the presence of oxygen. Oxygen could be consumed by the photochemically generated Cu^I species being oxidized to Cu^{II}, which could then be regenerated by photochemical routes. Furthermore, Boyer and co-workers have advanced oxygen reduction strategies in PET-RAFT systems wherein singlet oxygen quenchers, such as ascorbic acid, could be used to consume oxygen.

The potential of photoinduced Fe-catalyzed ATRP was investigated in nondegassed solutions, i.e., in the presence of residual oxygen. Table 2 compares the results of the polymerization of MMA in degassed and nondegassed solutions using FeBr₃/TBABr catalyst under blue LEDs. The reaction employing $[MMA]/[EBPA]/[FeBr_3]/[TBABr] = 100/1/0.04/$ 0.04 reached 93% monomer conversion in a nondegassed solution. It was well-controlled, forming polymers with molecular weights in agreement with theoretical values and a relatively low D of 1.38 (entry 1, Table 2). In comparison, the reaction was faster in a degassed solution, and a lower D of 1.17 was achieved (entry 2, Table 2). Increasing the concentration of FeBr₃ to 1000 ppm enhanced the efficiency of the reaction in the presence of oxygen as high conversion was achieved with lower D of 1.20 (entry 3, Table 2). It is worth noting that the reactions conducted in a full, capped vial without empty space on the top were well-controlled. No polymerization was observed when the reaction was conducted in a vial with \sim 40–50 vol % air due to continuous diffusion of oxygen to the

To further evaluate the behavior of this system in the presence of oxygen, the kinetics of the polymerization of MMA was investigated. As shown in Figure 6, the reaction conducted in the presence of oxygen (nondegassed solution) proceeded in a slightly lower rate compared to a degassed solution (oxygenfree solution). Nevertheless, in both systems molecular weights

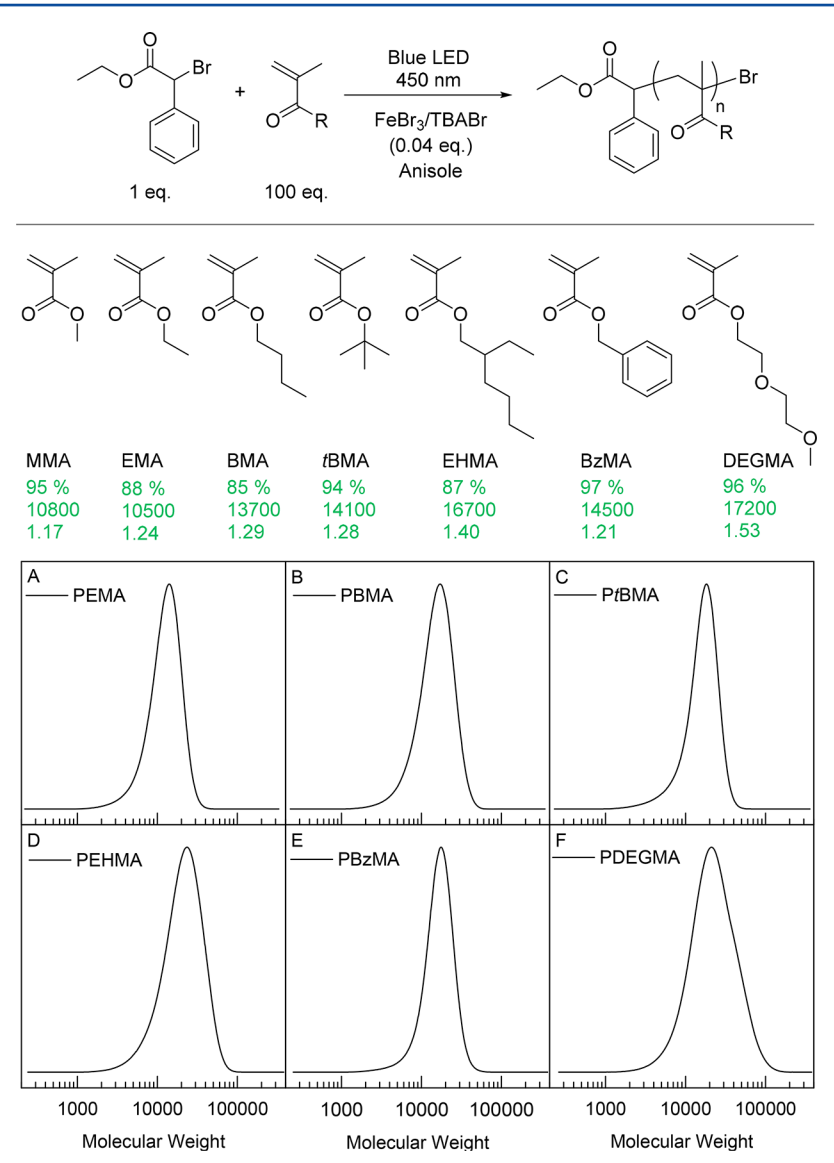


Figure 8. Monomers for the photoinduced Fe-catalyzed ATRP under blue light LED irradiation. Reaction conditions: $[M]/[EBPA]/[FeBr_3]/[TBABr] = 100/1/0.04/0.04$ in 50 vol % anisole, irradiated for 16 h. Numbers shown in green represent monomer conversion, $M_{n\nu}$ and D respectively from top to bottom.

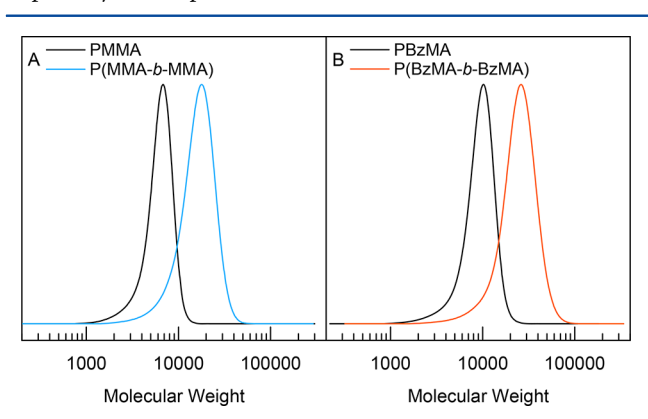


Figure 9. *In situ* chain extension of (A) PMMA with MMA and (B) PBzMA with BzMA in the photoinduced Fe-catalyzed ATRP under blue light LED irradiation. Reaction conditions for the synthesis of the macroinitiator: $[M]/[EBPA]/[FeBr_3]/[TBABr] = 50/1/0.04/0.04$ in 50 vol % anisole followed by the second addition of the monomer (100 equiv) and anisole *in situ*.

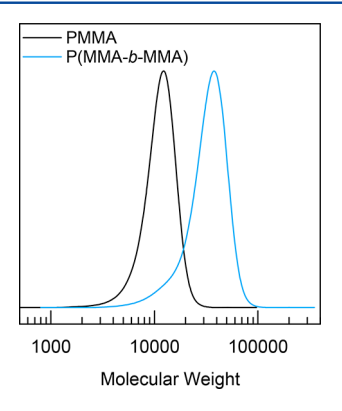


Figure 10. Chain extension of PMMA with MMA in the photoinduced Fe-catalyzed ATRP under blue light irradiation in the presence of oxygen.

increased as a function of monomer conversion, in good agreement with theoretical values and polymers with low $\cal D$ ranging from 1.17 to 1.25 were obtained. The slower rate of the

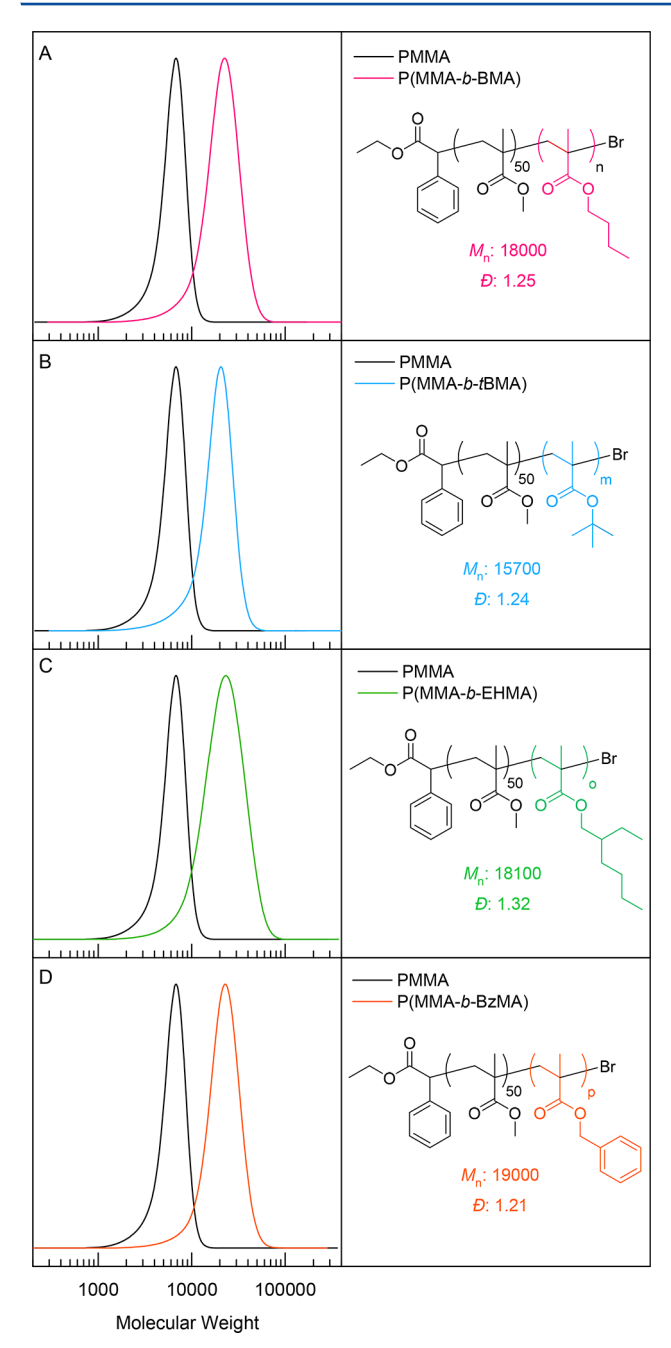


Figure 11. *In situ* block copolymerization of various methacrylate monomers in the photoinduced Fe-catalyzed ATRP under blue light LED irradiation. Reaction conditions for the synthesis of the PMMA macroinitiator: $[MMA]/[EBPA]/[FeBr_3]/[TBABr] = 50/1/0.04/0.04$ in 50 vol % anisole followed by the addition of the second monomer (100 equiv) and anisole *in situ*.

polymerization in the presence of oxygen could be attributed to the consumption of photochemically reduced FeBr₂ in reducing oxygen.

Varying Targeted DPs. Photoinduced Fe-catalyzed ATRP was applied to the polymerization of MMA with varying targeted degrees of polymerization (DP). As shown in Table 3 and Figure 7, MMA can be polymerized in a controlled manner with target DPs of 25, 50, 100, and 200. In all cases high monomer conversions (>90%) were reached with molecular weights in agreement with theoretical values while maintaining D as low as 1.17–1.25.

Range of Methacrylate Monomers. The scope of the photoinduced Fe-catalyzed ATRP initiated by visible light was explored for a variety of methacrylate monomers. As shown in Figure 8, monomers such as MMA, ethyl methacrylate (EMA), butyl methacrylate (BMA), tert-butyl methacrylate (tBMA), 2-ethylhexyl methacrylate (EHMA), benzyl methacrylate (BzMA), and di(ethylene glycol) methacrylate (DEGMA) were polymerized using FeBr₃/TBABr as the catalyst under blue light LED. Well-controlled polymers were obtained with all monomers tested with low D values (1.17–1.53) and high or near-quantitative monomer conversions (85–97%).

Ligands. Several ligands, including ionic, phosphine, and nitrogen-based ligands, were investigated in the Fe-catalyzed ATRP of MMA under blue light irradiation (Chart S1 and Table S1). A well-controlled process was observed using TBABr with near-quantitative monomer conversion and low Dof 1.17. Tetrabutylammonium triflate (TBATfO), which is a relatively weaker coordinating ligand than TBABr, also resulted in a controlled process with 88% monomer conversion and Dof 1.44. Phosphine ligands including tris(4-methoxyphenyl)phosphine (TMPP) and tris(2,4,6-trimethoxyphenyl)phosphine (TTMPP) showed excellent control in the polymerization of MMA with high or near-quantitative monomer conversion and low *Đ* of 1.20–1.29 (entries 3 and 4, Table S1). However, the nitrogen-based ligands were less efficient for the polymerization of MMA using FeBr₃ under blue light irradiation. Limited monomer conversions (<20%) were achieved while generating polymers with relatively high D (1.90 - 1.30)

Chain Extension and Block Copolymerization. Chain-end functionality of the polymers synthesized by the photoinduced Fe-ATRP was confirmed using ¹H NMR (Figure S1) by chain extension as well as by block copolymerization. A PMMA macroinitiator was synthesized under conditions [MMA]/ $[EBPA]/[FeBr_3]/[TBABr] = 50/1/0.04/0.04$ irradiating under blue light LEDs (conversion >95%, $M_{\rm p}$ = 5300, D = 1.17). The near-quantitative monomer conversion enabled in situ chain extension by addition of MMA in the second step without any further purification. Size-exclusion chromatography (SEC) analysis of the polymers presented in Figure 9 showed a clear shift toward higher molecular weights without any detectable shoulder or tailing at lower molecular weights ($M_p = 14\,000$, D= 1.22). To further demonstrate the versatility of this system, in situ chain extension was also examined for a PBzMA polymer obtained by photoinduced Fe-catalyzed ATRP under blue light irradiation. The initial PBzMA macroinitiator (conversion = 97%, $M_p = 8200$, D = 1.18) was successfully chain extended in situ with BzMA monomer in photoinduced Fe-catalyzed ATRP to yield P(BzMA-b-BzMA) $(M_n = 21\,000, D = 1.25)$ (Figure 9B).

Chain extension was further investigated in photoinduced Fe-catalyzed ATRP in the presence of oxygen. Initially, a PMMA macroinitiator was synthesized in the presence of oxygen under conditions [MMA]/[EBPA]/[FeBr₃]/[TBABr] = 100/1/0.1/0.1 in 50 vol % anisole under blue LED to yield PMMA with M_n = $10\,300$ and D = 1.14. Chain extension was performed using the above PMMA-Br macroinitiator in photoinduced Fe-catalyzed ATRP in the presence of oxygen under conditions: [MMA]/[PMMA-Br]/[FeBr₃]/[TBABr] = 200/1/0.1/0.1 in 50 vol % anisole. SEC results shown in Figure 10 indicated a successful chain extension of the PMMA to higher molecular weights using photoinduced Fe-catalyzed ATRP in the presence of oxygen (M_n = $28\,400$, D = 1.23).

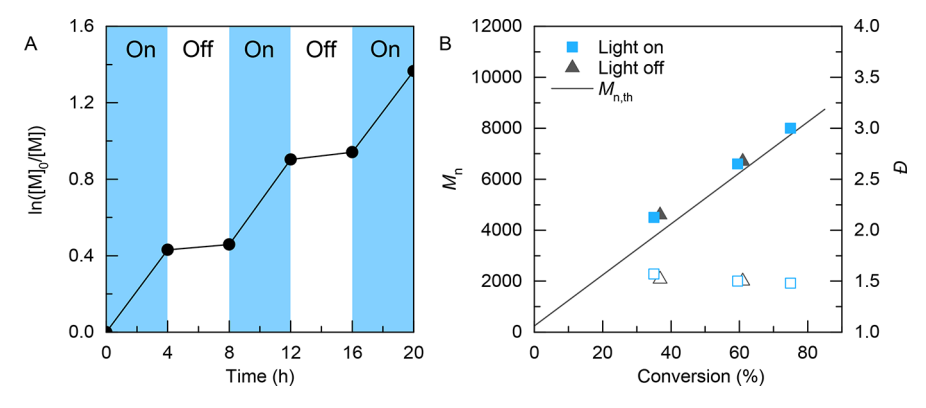


Figure 12. Temporal control of the photoinduced Fe-catalyzed ATRP under blue light LED irradiation. (A) Kinetics and (B) molecular weight and dispersity as a function of monomer conversion. Reaction conditions: [MMA]/[EBPA]/[FeBr₃]/[TBABr] = 100/1/0.02/0.02 in 50 vol % anisole.

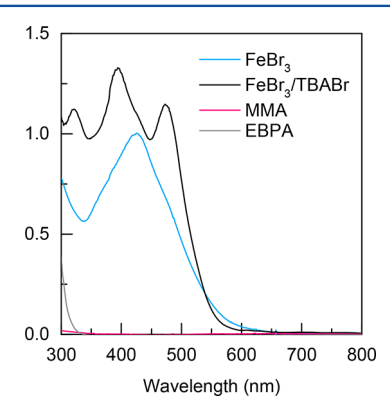


Figure 13. UV—vis spectra of FeBr₃, FeBr₃/TBABr, MMA, and EBPA in anisole. Concentrations: 0.2 mM.

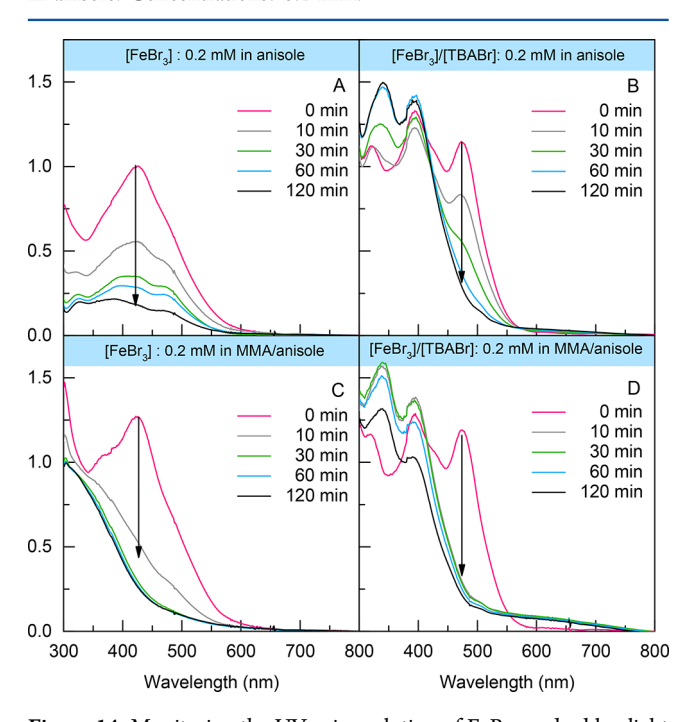
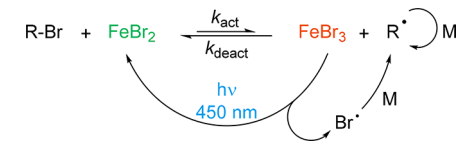


Figure 14. Monitoring the UV—vis evolution of $FeBr_3$ under blue light LED irradiation as a function of time.

Subsequently, in situ block copolymerization was also attempted, and various block copolymers were synthesized with a PMMA macroinitiator (conversion >95%, M_n = 5300, D = 1.17), followed by sequential addition of a degassed solution

Scheme 1. Proposed Mechanism for Photoinduced Fe-Catalyzed ATRP



of the second monomer (100 equiv) in 50 vol % anisole. Monomers including BMA, tBMA, EHMA, and BzMA were successfully used in the in situ block copolymerization in photoinduced Fe-ATRP. SEC traces showed a shift to higher molecular weights in the block copolymerizations, while copolymers maintained low D (1.20–1.30), indicating high chain-end functionality under blue light LEDs (Figure 11 and Figure S2).

Temporal Control. Temporal control experiments were performed by switching the blue light on/off intermittently. The kinetic results showed the polymerization of MMA in the presence of FeBr₃/TBABr proceeding under blue light whereas the rate of the reaction was significantly reduced when the light was turned off. Re-exposing the solution to blue light in the second light-on period restarted the reaction to reach higher conversions. Control was maintained throughout successive on/off periods with molecular weights in agreement with theoretical values and low *D*. As shown in Figure 12, temporal control enabled successful manipulation of the polymerization using FeBr₃ catalyst under blue light.

UV-Vis Spectroscopic Studies and Photoreduction Mechanism. The UV-vis spectra of the polymerization components including FeBr3, TBABr, MMA, and EBPA were recorded and are shown in Figure 13. The FeBr₃/TBABr complex exhibits strong, broad absorption from UV up to visible region extending to green light, whereas other components are completely transparent in this region. To better understand the photoreduction mechanism, the UV-vis spectra of the catalytic system were recorded under different conditions. As shown in Figure 14A, a solution of FeBr₃ in anisole showed a reduction in the absorption peak of FeBe₃ above 400 nm under blue light LED irradiation. In the presence of MMA, the reduction of the FeBr₃ peak was much faster (Figure 14B). A similar trend was also observed when FeBr₃ was complexed with TBABr ligand with a faster reduction of FeBr₃ in the presence of MMA (Figure 14C vs 14D). These results suggest that MMA is involved in the reduction of FeBr₃, as previously reported. 66,77,78

Two possible mechanisms can be considered for the reduction of FeBr₃. One pathway involves the homolytic photolysis of an Fe-Br bond under irradiation, yielding FeBr₂ and a Br radical. Another pathway could be MMA-mediated reduction of FeBr₂, which in turn forms FeBr₂ and an alkyl halide initiator, methyl 2,3-dibromoisobutyrate. To prove whether or not the homolytic Fe-Br bond cleavage was the dominant pathway, a series of control experiments were performed using iron(III) triflate (Fe(OTf)₃) instead of FeBr₃, with noncoordinating triflate anions. Control experiments in the presence of Fe(OTf)3 and TBABr ligand indicated 15% monomer conversion after 24 h irradiation under blue light ($M_p = 11\,300$, D = 2.70). However, changing the ligand to TBAOTf or TTMPP in the presence or absence of EBPA initiator gave no monomer conversion during 24 h under blue light. The lack of polymerization in the presence of Fe(OTf)₃ and non-Br ligands suggests that homolytic Fe-Br bond photolysis plays an important role in reduction of FeBr₃.

Therefore, the plausible mechanism should involve unimolecular Fe—Br cleavage under light, which forms FeBr₂ and Br[•] radical (Scheme 1). While FeBr₂ can activate alkyl halide to initiate polymerization, the Br[•] radical can also add to the monomer and initiate polymerization. The 3-bromoisobuytryl radical thus-formed can then be deactivated by FeBr₃ present in the system generating methyl 2,3-dibromoisobutyrate and FeBr₂. This should be the reason for the faster reduction of FeBr₃ in the presence of MMA, as shown in Figure 14.

CONCLUSION

Fe-catalyzed ATRP of methacrylate monomers can be promoted with an excellent control under blue LED irradiation. Because of the broad optical absorption of FeBr₃ catalyst, a wide range of light sources from UV to blue and to green lights can be applied. Well-controlled polymers were synthesized with predetermined molecular weight and low dispersity. Excellent retention of chain-end functionality was confirmed by successful formation of block copolymers *in situ*. Furthermore, photocatalytic reduction of oxygen allows for promotion of well-controlled polymerization in the presence of oxygen. The ubiquity and biocompatibility of photocatalytically active Fe species suggest them as promising, inexpensive, green catalysts for ATRP systems.

ASSOCIATED CONTENT

S Supporting Information

The Supporting Information is available free of charge on the ACS Publications website at DOI: 10.1021/acs.macromol.7b01708.

Experimental procedures, additional polymerization results, and 1H NMR spectra (PDF)

■ AUTHOR INFORMATION

Corresponding Author

*E-mail: km3b@andrew.cmu.edu (K.M.).

ORCID ®

Sajjad Dadashi-Silab: 0000-0002-4285-5846 Xiangcheng Pan: 0000-0003-3344-4639

Krzysztof Matyjaszewski: 0000-0003-1960-3402

Notes

The authors declare no competing financial interest.

ACKNOWLEDGMENTS

We thank the NSF (CHE-1707490) for the financial support. X.P. acknowledges the support from the National Natural Science Foundation of China (21704017).

REFERENCES

- (1) Wang, J. S.; Matyjaszewski, K. Controlled Living Radical Polymerization Atom-Transfer Radical Polymerization in the Presence of Transition-Metal Complexes. *J. Am. Chem. Soc.* **1995**, 117, 5614–5615.
- (2) Matyjaszewski, K.; Xia, J. H. Atom transfer radical polymerization. *Chem. Rev.* **2001**, *101*, 2921–2990.
- (3) Kamigaito, M.; Ando, T.; Sawamoto, M. Metal-Catalyzed Living Radical Polymerization. *Chem. Rev.* **2001**, *101*, 3689–3746.
- (4) Matyjaszewski, K. Atom Transfer Radical Polymerization (ATRP): Current Status and Future Perspectives. *Macromolecules* **2012**, *45*, 4015–4039.
- (5) Matyjaszewski, K.; Tsarevsky, N. V. Macromolecular Engineering by Atom Transfer Radical Polymerization. *J. Am. Chem. Soc.* **2014**, *136*, 6513–6533.
- (6) Moad, G.; Rizzardo, E.; Thang, S. H. Living Radical Polymerization by the RAFT Process A Third Update. *Aust. J. Chem.* **2012**, *65*, 985–1076.
- (7) Hawker, C. J.; Bosman, A. W.; Harth, E. New polymer synthesis by nitroxide mediated living radical polymerizations. *Chem. Rev.* **2001**, *101*, 3661–3688.
- (8) Nicolas, J.; Guillaneuf, Y.; Lefay, C.; Bertin, D.; Gigmes, D.; Charleux, B. Nitroxide-mediated polymerization. *Prog. Polym. Sci.* **2013**, 38, 63–235.
- (9) Tebben, L.; Studer, A. Nitroxides: Applications in Synthesis and in Polymer Chemistry. *Angew. Chem., Int. Ed.* **2011**, *50*, 5034–5068.
- (10) Krys, P.; Matyjaszewski, K. Kinetics of Atom Transfer Radical Polymerization. *Eur. Polym. J.* **2017**, *89*, 482–523.
- (11) di Lena, F.; Matyjaszewski, K. Transition metal catalysts for controlled radical polymerization. *Prog. Polym. Sci.* **2010**, *35*, 959–1021.
- (12) Matyjaszewski, K.; Jakubowski, W.; Min, K.; Tang, W.; Huang, J.; Braunecker, W. A.; Tsarevsky, N. V. Diminishing catalyst concentration in atom transfer radical polymerization with reducing agents. *Proc. Natl. Acad. Sci. U. S. A.* **2006**, *103*, 15309–15314.
- (13) Konkolewicz, D.; Magenau, A. J. D.; Averick, S. E.; Simakova, A.; He, H. K.; Matyjaszewski, K. ICAR ATRP with ppm Cu Catalyst in Water. *Macromolecules* **2012**, *45*, 4461–4468.
- (14) Min, K.; Gao, H. F.; Matyjaszewski, K. Preparation of homopolymers and block copolymers in miniemulsion by ATRP using activators generated by electron transfer (AGET). *J. Am. Chem. Soc.* **2005**, 127, 3825–3830.
- (15) Jakubowski, W.; Matyjaszewski, K. Activators regenerated by electron transfer for atom-transfer radical polymerization of (meth)-acrylates and related block copolymers. *Angew. Chem., Int. Ed.* **2006**, 45, 4482–4486.
- (16) Konkolewicz, D.; Wang, Y.; Zhong, M. J.; Krys, P.; Isse, A. A.; Gennaro, A.; Matyjaszewski, K. Reversible-Deactivation Radical Polymerization in the Presence of Metallic Copper. A Critical Assessment of the SARA ATRP and SET-LRP Mechanisms. *Macromolecules* **2013**, *46*, 8749–8772.
- (17) Matyjaszewski, K.; Coca, S.; Gaynor, S. G.; Wei, M. L.; Woodworth, B. E. Zerovalent metals in controlled "living" radical polymerization. *Macromolecules* **1997**, *30*, 7348–7350.
- (18) Anastasaki, A.; Nikolaou, V.; Nurumbetov, G.; Wilson, P.; Kempe, K.; Quinn, J. F.; Davis, T. P.; Whittaker, M. R.; Haddleton, D. M. Cu(0)-Mediated Living Radical Polymerization: A Versatile Tool for Materials Synthesis. *Chem. Rev.* **2016**, *116*, 835–877.
- (19) Boyer, C.; Corrigan, N. A.; Jung, K.; Nguyen, D.; Nguyen, T. K.; Adnan, N. N. M.; Oliver, S.; Shanmugam, S.; Yeow, J. Copper-Mediated Living Radical Polymerization (Atom Transfer Radical Polymerization and Copper(0) Mediated Polymerization): From Fundamentals to Bioapplications. *Chem. Rev.* **2016**, *116*, 1803–1949.

(20) Magenau, A. J. D.; Strandwitz, N. C.; Gennaro, A.; Matyjaszewski, K. Electrochemically Mediated Atom Transfer Radical Polymerization. *Science* **2011**, 332, 81–84.

- (21) Li, B.; Yu, B.; Huck, W. T. S.; Zhou, F.; Liu, W. Electrochemically Induced Surface-Initiated Atom-Transfer Radical Polymerization. *Angew. Chem., Int. Ed.* **2012**, *51*, 5092–5095.
- (22) Li, B.; Yu, B.; Huck, W. T. S.; Liu, W.; Zhou, F. Electrochemically Mediated Atom Transfer Radical Polymerization on Nonconducting Substrates: Controlled Brush Growth through Catalyst Diffusion. *J. Am. Chem. Soc.* **2013**, *135*, 1708–1710.
- (23) Shida, N.; Koizumi, Y.; Nishiyama, H.; Tomita, I.; Inagi, S. Electrochemically Mediated Atom Transfer Radical Polymerization from a Substrate Surface Manipulated by Bipolar Electrolysis: Fabrication of Gradient and Patterned Polymer Brushes. *Angew. Chem., Int. Ed.* **2015**, *54*, 3922–3926.
- (24) Chmielarz, P.; Fantin, M.; Park, S.; Isse, A. A.; Gennaro, A.; Magenau, A. J. D.; Sobkowiak, A.; Matyjaszewski, K. Electrochemically mediated atom transfer radical polymerization (eATRP). *Prog. Polym. Sci.* **2017**, *69*, 47–78.
- (25) Tasdelen, M. A.; Uygun, M.; Yagci, Y. Photoinduced Controlled Radical Polymerization in Methanol. *Macromol. Chem. Phys.* **2010**, *211*, 2271–2275.
- (26) Tasdelen, M. A.; Uygun, M.; Yagci, Y. Photoinduced Controlled Radical Polymerization. *Macromol. Rapid Commun.* **2011**, 32, 58–62.
- (27) Mosnáček, J.; Ilčíková, M. Photochemically Mediated Atom Transfer Radical Polymerization of Methyl Methacrylate Using ppm Amounts of Catalyst. *Macromolecules* **2012**, *45*, 5859–5865.
- (28) Konkolewicz, D.; Schröder, K.; Buback, J.; Bernhard, S.; Matyjaszewski, K. Visible Light and Sunlight Photoinduced ATRP with ppm of Cu Catalyst. ACS Macro Lett. 2012, 1, 1219–1223.
- (29) Anastasaki, A.; Nikolaou, V.; Zhang, Q.; Burns, J.; Samanta, S. R.; Waldron, C.; Haddleton, A. J.; McHale, R.; Fox, D.; Percec, V.; Wilson, P.; Haddleton, D. M. Copper(II)/Tertiary Amine Synergy in Photoinduced Living Radical Polymerization: Accelerated Synthesis of ω -Functional and α , ω -Heterofunctional Poly(acrylates). *J. Am. Chem. Soc.* **2014**, *136*, 1141–1149.
- (30) Ribelli, T. G.; Konkolewicz, D.; Bernhard, S.; Matyjaszewski, K. How are Radicals (Re)Generated in Photochemical ATRP? *J. Am. Chem. Soc.* **2014**, *136*, 13303–13312.
- (31) Dadashi-Silab, S.; Tasdelen, M. A.; Kiskan, B.; Wang, X.; Antonietti, M.; Yagci, Y. Photochemically Mediated Atom Transfer Radical Polymerization Using Polymeric Semiconductor Mesoporous Graphitic Carbon Nitride. *Macromol. Chem. Phys.* **2014**, 215, 675–681.
- (32) Fors, B. P.; Hawker, C. J. Control of a Living Radical Polymerization of Methacrylates by Light. *Angew. Chem., Int. Ed.* **2012**, *51*, 8850–8853.
- (33) Discekici, E. H.; Anastasaki, A.; Kaminker, R.; Willenbacher, J.; Truong, N. P.; Fleischmann, C.; Oschmann, B.; Lunn, D. J.; Read de Alaniz, J.; Davis, T. P.; Bates, C. M.; Hawker, C. J. Light-Mediated Atom Transfer Radical Polymerization of Semi-Fluorinated (Meth)acrylates: Facile Access to Functional Materials. *J. Am. Chem. Soc.* 2017, 139, 5939–5945.
- (34) Mohapatra, H.; Kleiman, M.; Esser-Kahn, A. P. Mechanically controlled radical polymerization initiated by ultrasound. *Nat. Chem.* **2017**, *9*, 135–139.
- (35) Wang, Z.; Pan, X.; Yan, J.; Dadashi-Silab, S.; Xie, G.; Zhang, J.; Wang, Z.; Xia, H.; Matyjaszewski, K. Temporal Control in Mechanically Controlled Atom Transfer Radical Polymerization Using Low ppm of Cu Catalyst. ACS Macro Lett. 2017, 6, 546–549.
- (36) Dadashi-Silab, S.; Doran, S.; Yagci, Y. Photoinduced Electron Transfer Reactions for Macromolecular Syntheses. *Chem. Rev.* **2016**, *116*, 10212–10275.
- (37) Chen, M.; Zhong, M. J.; Johnson, J. A. Light-Controlled Radical Polymerization: Mechanisms, Methods, and Applications. *Chem. Rev.* **2016**, *116*, 10167–10211.
- (38) Pan, X.; Tasdelen, M. A.; Laun, J.; Junkers, T.; Yagci, Y.; Matyjaszewski, K. Photomediated controlled radical polymerization. *Prog. Polym. Sci.* **2016**, *62*, 73–125.

(39) Corrigan, N.; Shanmugam, S.; Xu, J.; Boyer, C. Photocatalysis in organic and polymer synthesis. *Chem. Soc. Rev.* **2016**, *45*, 6165–6212.

- (40) Shanmugam, S.; Xu, J.; Boyer, C. Photocontrolled Living Polymerization Systems with Reversible Deactivations through Electron and Energy Transfer. *Macromol. Rapid Commun.* **2017**, 38, 1700143.
- (41) Dadashi-Silab, S.; Tasdelen, M. A.; Yagci, Y. Photoinitiated Atom Transfer Radical Polymerization: Current Status and Future Perspectives. J. Polym. Sci., Part A: Polym. Chem. 2014, 52, 2878–2888.
- (42) Treat, N. J.; Fors, B. P.; Kramer, J. W.; Christianson, M.; Chiu, C.-Y.; Read de Alaniz, J.; Hawker, C. J. Controlled Radical Polymerization of Acrylates Regulated by Visible Light. *ACS Macro Lett.* **2014**, *3*, 580–584.
- (43) Theriot, J. C.; McCarthy, B. G.; Lim, C.-H.; Miyake, G. M. Organocatalyzed Atom Transfer Radical Polymerization: Perspectives on Catalyst Design and Performance. *Macromol. Rapid Commun.* **2017**, 38, 1700040.
- (44) Treat, N. J.; Sprafke, H.; Kramer, J. W.; Clark, P. G.; Barton, B. E.; Read de Alaniz, J.; Fors, B. P.; Hawker, C. J. Metal-Free Atom Transfer Radical Polymerization. *J. Am. Chem. Soc.* **2014**, *136*, 16096—16101.
- (45) Pan, X.; Lamson, M.; Yan, J.; Matyjaszewski, K. Photoinduced Metal-Free Atom Transfer Radical Polymerization of Acrylonitrile. *ACS Macro Lett.* **2015**, *4*, 192–196.
- (46) Pan, X.; Fang, C.; Fantin, M.; Malhotra, N.; So, W. Y.; Peteanu, L. A.; Isse, A. A.; Gennaro, A.; Liu, P.; Matyjaszewski, K. Mechanism of Photoinduced Metal-Free Atom Transfer Radical Polymerization: Experimental and Computational Studies. *J. Am. Chem. Soc.* **2016**, *138*, 2411–2425.
- (47) Theriot, J. C.; Lim, C.-H.; Yang, H.; Ryan, M. D.; Musgrave, C. B.; Miyake, G. M. Organocatalyzed atom transfer radical polymerization driven by visible light. *Science* **2016**, 352, 1082–1086.
- (48) Pan, X.; Malhotra, N.; Dadashi-Silab, S.; Matyjaszewski, K. A Simplified Fe-Based PhotoATRP Using Only Monomers and Solvent. *Macromol. Rapid Commun.* **2017**, *38*, 1600651.
- (49) Matyjaszewski, K.; Wei, M.; Xia, J.; McDermott, N. E. Controlled/"Living" Radical Polymerization of Styrene and Methyl Methacrylate Catalyzed by Iron Complexes. *Macromolecules* **1997**, *30*, 8161–8164.
- (50) Ando, T.; Kamigaito, M.; Sawamoto, M. Iron(II) Chloride Complex for Living Radical Polymerization of Methyl Methacrylate. *Macromolecules* **1997**, 30, 4507–4510.
- (51) Allan, L. E. N.; MacDonald, J. P.; Nichol, G. S.; Shaver, M. P. Single Component Iron Catalysts for Atom Transfer and Organometallic Mediated Radical Polymerizations: Mechanistic Studies and Reaction Scope. *Macromolecules* **2014**, *47*, 1249–1257.
- (52) Xue, Ž.; He, D.; Xie, X. Iron-catalyzed atom transfer radical polymerization. *Polym. Chem.* **2015**, *6*, 1660–1687.
- (53) Poli, R.; Allan, L. E. N.; Shaver, M. P. Iron-mediated reversible deactivation controlled radical polymerization. *Prog. Polym. Sci.* **2014**, 39, 1827–1845.
- (54) Bauer, I.; Knölker, H.-J. Iron Catalysis in Organic Synthesis. Chem. Rev. 2015, 115, 3170-3387.
- (55) Niibayashi, S.; Hayakawa, H.; Jin, R.-H.; Nagashima, H. Reusable and environmentally friendly ionic trinuclear iron complex catalyst for atom transfer radical polymerization. *Chem. Commun.* **2007**, 1855–1857.
- (56) Allan, L. E. N.; MacDonald, J. P.; Reckling, A. M.; Kozak, C. M.; Shaver, M. P. Controlled Radical Polymerization Mediated by Amine—Bis(phenolate) Iron(III) Complexes. *Macromol. Rapid Commun.* **2012**, 33, 414–418.
- (57) Schroeder, H.; Lake, B. R. M.; Demeshko, S.; Shaver, M. P.; Buback, M. A Synthetic and Multispectroscopic Speciation Analysis of Controlled Radical Polymerization Mediated by Amine—Bis-(phenolate)iron Complexes. *Macromolecules* **2015**, *48*, 4329–4338.
- (58) Xue, Z.; Linh, N. T. B.; Noh, S. K.; Lyoo, W. S. Phosphorus-Containing Ligands for Iron(III)-Catalyzed Atom Transfer Radical Polymerization. *Angew. Chem., Int. Ed.* **2008**, *47*, 6426–6429.

(59) Wang, Y.; Kwak, Y.; Matyjaszewski, K. Enhanced Activity of ATRP Fe Catalysts with Phosphines Containing Electron Donating Groups. *Macromolecules* **2012**, *45*, 5911–5915.

- (60) Nishizawa, K.; Ouchi, M.; Sawamoto, M. Phosphine–Ligand Decoration toward Active and Robust Iron Catalysts in LRP. *Macromolecules* **2013**, *46*, 3342–3349.
- (61) Xue, Z.; Oh, H. S.; Noh, S. K.; Lyoo, W. S. Phosphorus Ligands for Iron(III)-Mediated Atom Transfer Radical Polymerization of Methyl Methacrylate. *Macromol. Rapid Commun.* **2008**, *29*, 1887—1894.
- (62) Teodorescu, M.; Gaynor, S. G.; Matyjaszewski, K. Halide Anions as Ligands in Iron-Mediated Atom Transfer Radical Polymerization. *Macromolecules* **2000**, *33*, 2335–2339.
- (63) Wang, Y.; Matyjaszewski, K. ATRP of MMA Catalyzed by FeIIBr2 in the Presence of Triflate Anions. *Macromolecules* **2011**, *44*, 1226–1228.
- (64) Wang, Y.; Zhang, Y.; Parker, B.; Matyjaszewski, K. ATRP of MMA with ppm Levels of Iron Catalyst. *Macromolecules* **2011**, *44*, 4022–4025.
- (65) Wang, Y.; Matyjaszewski, K. ATRP of MMA in Polar Solvents Catalyzed by FeBr2 without Additional Ligand. *Macromolecules* **2010**, 43, 4003–4005.
- (66) Pan, X.; Malhotra, N.; Zhang, J.; Matyjaszewski, K. Photo-induced Fe-Based Atom Transfer Radical Polymerization in the Absence of Additional Ligands, Reducing Agents, and Radical Initiators. *Macromolecules* **2015**, *48*, 6948–6954.
- (67) Zhou, Y.-N.; Guo, J.-K.; Li, J.-J.; Luo, Z.-H. Photoinduced Iron(III)-Mediated Atom Transfer Radical Polymerization with In Situ Generated Initiator: Mechanism and Kinetics Studies. *Ind. Eng. Chem. Res.* **2016**, *55*, 10235–10242.
- (68) Telitel, S.; Dumur, F.; Campolo, D.; Poly, J.; Gigmes, D.; Pierre Fouassier, J.; Lalevée, J. Iron complexes as potential photocatalysts for controlled radical photopolymerizations: A tool for modifications and patterning of surfaces. *J. Polym. Sci., Part A: Polym. Chem.* **2016**, *54*, 702–713.
- (69) Ligon, S. C.; Husár, B.; Wutzel, H.; Holman, R.; Liska, R. Strategies to Reduce Oxygen Inhibition in Photoinduced Polymerization. *Chem. Rev.* **2014**, *114*, 557–589.
- (70) Mosnacek, J.; Eckstein-Andicsova, A.; Borska, K. Ligand effect and oxygen tolerance studies in photochemically induced copper mediated reversible deactivation radical polymerization of methyl methacrylate in dimethyl sulfoxide. *Polym. Chem.* **2015**, *6*, 2523–2530.
- (71) Yang, Q.; Lalevée, J.; Poly, J. Development of a Robust Photocatalyzed ATRP Mechanism Exhibiting Good Tolerance to Oxygen and Inhibitors. *Macromolecules* **2016**, 49, 7653–7666.
- (72) Pan, X.; Lathwal, S.; Mack, S.; Yan, J.; Das, S. R.; Matyjaszewski, K. Automated Synthesis of Well-Defined Polymers and Biohybrids by Atom Transfer Radical Polymerization Using a DNA Synthesizer. *Angew. Chem., Int. Ed.* **2017**, *56*, 2740–2743.
- (73) Borská, K.; Moravčíková, D.; Mosnáček, J. Photochemically Induced ATRP of (Meth)Acrylates in the Presence of Air: The Effect of Light Intensity, Ligand, and Oxygen Concentration. *Macromol. Rapid Commun.* **2017**, *38*, 1600639.
- (74) Shanmugam, S.; Xu, J.; Boyer, C. Aqueous RAFT Photopolymerization with Oxygen Tolerance. *Macromolecules* **2016**, *49*, 9345–9357.
- (75) Yeow, J.; Chapman, R.; Xu, J.; Boyer, C. Oxygen tolerant photopolymerization for ultralow volumes. *Polym. Chem.* **2017**, 8, 5012–5022.
- (76) Shanmugam, S.; Xu, J.; Boyer, C. Photoinduced Oxygen Reduction for Dark Polymerization. *Macromolecules* **2017**, *50*, 1832–1846.
- (77) Xue, Z.; He, D.; Noh, S. K.; Lyoo, W. S. Iron(III)-Mediated Atom Transfer Radical Polymerization in the Absence of Any Additives. *Macromolecules* **2009**, 42, 2949–2957.
- (78) Khan, M. Y.; Chen, X.; Lee, S. W.; Noh, S. K. Development of New Atom Transfer Radical Polymerization System by Iron (III)-Metal Salts Without Using any External Initiator and Reducing Agent. *Macromol. Rapid Commun.* **2013**, 34, 1225–1230.